Assessing the Potential of Fully Polarimetric Mono- and Bistatic SAR Acquisitions in L-Band for Crop and Soil Monitoring

Jean Bouchat, Emma Tronquo, Anne Orban, Niko E. C. Verhoest, and Pierre Defourny, *Member, IEEE*

***Abstract*—Theoretical studies have shown that the use of simultaneous mono- and bistatic synthetic aperture radar (SAR) data could be beneficial to agriculture and soil moisture monitoring. This study makes use of extensive ground-truth measurements and synchronous high-resolution fully polarimetric mono- and bistatic airborne SAR data in L-band to assess and compare the sensitivity of mono- and multistatic systems to the maize canopy row structure and biophysical variables, as well as to soil moisture and surface roughness in both vegetated and bare fields. The effect of the row structure of maize crops is assessed through the impact of the orientation of the planting rows relative to the sensor beam on microwave scattering measurements. The results of this analysis suggest that the row orientation of maize crops has a significant influence on both mono- and bistatic scattering measurements in both copolarizations, and especially, in HH, while the cross polarizations are not affected. Furthermore, the study also shows through a linear regression analysis that bistatic data, even with a very small bistatic baseline, can provide valuable additional information for maize crop biophysical variable retrieval, which however does not appear to be the case for soil moisture retrieval over bare soils.**

***Index Terms*—Agriculture, biophysical variables, bistatic synthetic aperture radar (SAR), L-band, maize, row structure, soil moisture.**

I. Introduction

BISTATIC synthetic aperture radars (SARs) are radar systems in which the transmitter and receiver are physically separated, as opposed to monostatic systems in which they share the same location. Multistatic systems, meanwhile, have multiple receivers to a common transmitter. These systems allow for the acquisition of images using various geometries and configurations, thereby, capturing multidimensional scattering effects that could not be recorded by monostatic systems alone.

In agricultural areas, radar measurements are influenced by both vegetation and underlying soil, as well as their interactions, making it difficult to differentiate between their respective contributions. The use of a second receiver in addition to a conventional monostatic system, i.e., transmitter–receiver, forming a multistatic system, could improve the retrieval performance of vegetation and soil biogeophysical variables.

With regard to the former, multiple theoretical investigations into the scattering behavior of microwaves in agricultural areas have demonstrated that certain bistatic sensor configurations could limit the contribution of the underlying soil to the recorded scattering, thus making it possible to better distinguish the signature of the vegetation in the scattered signal and improve the retrieval accuracy of vegetation biophysical variables [1]–[3]. These model-based studies, aimed at identifying the optimal bistatic configuration for biophysical variables retrieval from L-band SAR data, have demonstrated that the passive sensor should ideally be in the plane that lies in azimuth angle orthogonal to the plane of incidence [2] and with a very large bistatic baseline [3].

Regarding the latter, studies by Schmugge [4] and Ulaby *et al.* [5], [6] illustrated that in agricultural areas, the scattered microwave signal is partially influenced by the dielectric properties of the soil, and thus, the soil moisture content. Furthermore, since the radar signal is also highly sensitive to the geometric arrangement of scatterers on the ground surface, the radar measurements are not only sensitive to soil moisture, but also to soil surface roughness, which is commonly affected by tillage operations in agricultural fields [7], [8]. As a result, it is difficult to differentiate between the contributions of soil moisture and surface roughness on radar backscatter when relying on measurements from monostatic SAR systems alone. This makes the retrieval of soil moisture with such systems challenging. Recent studies investigated the potential of combining radar and optical images, from Sentinel-1 and Sentinel-2, respectively, for predicting soil moisture and crop biophysical parameters [9]–[11]. The results of these studies show that combining the microwave and optical domains is a promising technique for finer crop and soil monitoring thanks to an increased temporal sampling and retrieval accuracy. Furthermore, the interest in bistatic and multistatic radar remote sensing has grown over recent years, whereby several studies reported an expected mitigation of the adverse

Manuscript received December 31, 2021; revised March 4, 2022; accepted March 22, 2022. Date of publication March 29, 2022; date of current version May 3, 2022. This article was presented in part at the 2021 IEEE International Geoscience and Remote Sensing Symposium (IGARSS), Virtual Symposium, Brussels, Belgium, July 2021. This work was supported in part by the STEREO III program of the Belgian Federal Science Policy Office (BELSPO) under Contract SR/00/371 and in part by the PRODEX program of the European Space Agency (ESA) under Contract 4000130658. *(Corresponding author: Jean Bouchat.)*

Jean Bouchat and Pierre Defourny are with the Earth and Life Institute, Université catholique de Louvain, 1348 Louvain-la-Neuve, Belgium (e-mail: jean.bouchat@uclouvain.be; pierre.defourny@uclouvain.be).

Emma Tronquo and Niko E. C. Verhoest are with the Hydro-Climate Extremes Lab (H-CEL), Ghent University, 9000 Ghent, Belgium (e-mail: emma.tronquo@ugent.be; niko.verhoest@ugent.be).

Anne Orban is with the Centre Spatial de Liège, Université de Liège, 4031 Angleur, Belgium (e-mail: aorban@uliege.be).

Digital Object Identifier 10.1109/JSTARS.2022.3162911

impact of surface roughness on the retrieval of soil moisture with the simultaneous use of mono- and bistatic SAR scattering data, i.e., multistatic [12]–[17]. Global navigation satellite signal reflectometry (GNSS-R) is a bistatic remote sensing technique that has been studied extensively over recent years, by means of both theoretical modeling and experimental results [18], [19]. One of the main drawbacks of these GNSS-R studies is the fact they are focused on bistatic scattering in the specular region. In order to evaluate various SAR geometries for soil moisture detection, only studies relying on theoretical model simulations are available to-date, e.g., [13] and [15]. In these studies, it is hypothesized that the impact of surface roughness can be mitigated with the use of two simultaneous observations of the scene. The results of these works point to an improvement in soil moisture retrieval accuracy, especially for bistatic measurements performed in the forward region [3], [13], [20].

Despite these considerable expected advantages, the number and importance of bistatic SAR applications for vegetation and soil monitoring have remained low. It seems that this scarcity can be in part attributed to a lack of experimental datasets combining mono- and bistatic SAR acquisitions and *in situ* measurements of vegetation and soil biogeophysical variables.

This study, which builds on [21] and [22], uses one of the very first high-resolution fully polarimetric mono- and bistatic SAR datasets in L-band ever acquired to assess the potential of simultaneous mono- and bistatic SAR acquisitions for agriculture and soil moisture monitoring applications. To that end, this study aims to evaluate their sensitivity to maize crop biophysical variables and canopy row structure, as well as to the soil moisture and surface roughness in vegetated and bare agricultural fields.

II. Data

A. Site Description

The BELSAR airborne and field campaign took place during the 2018 growing season, between May and September, in the Hesbania BELAIR test site, between Gembloux and Sint-Truiden. The site, in Fig. 2, which corresponds, which corresponds to a typical landscape of intensive agriculture of Belgium, belongs to the global JECAM network. It is mostly covered by relatively large, homogeneous, and flat fields with a uniform topsoil texture of silt loam.

B. Airborne SAR Data

The radar data for this study were collected during a series of five flight missions with two airplanes carrying a multistatic SAR system. The flights took place approximately one month apart, between May 31 and September 10, 2018.

Mono- and bistatic airborne radar data were acquired simultaneously by two left-looking L-band SAR operated by MetaSensing BV on-board two CESNA Gran Caravan specifically adapted for the mission. The radar systems and planes are shown on Fig. 1.

MetaSensing BV's airborne L-band SAR system [23] is a versatile compact sensor providing imaging with spatial resolution up to 1 m, equipped with two flat antennas: a squared one

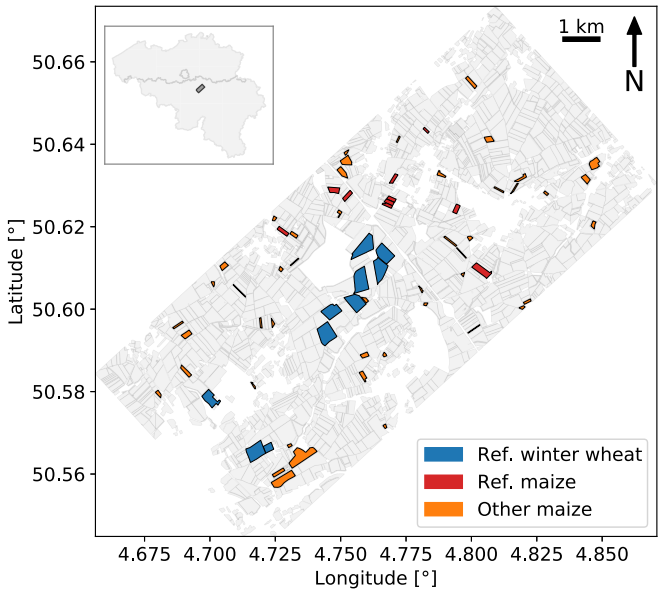

Fig. 2. BELSAR area of interest, with the reference winter wheat and maize fields in which the *in situ* measurements were acquired in blue and red, respectively, other maize fields in the area in orange, and all the other agricultural fields inventoried as delineated in the Land Parcel Information System of Wallonia, Belgium, in gray.

Fig. 1. MetaSensing BV's airborne L-band SAR system on-board one of the two CESNA Gran Caravan airplanes (left) and a picture of one airplane taken from the other while flying in the across-track (XT) configuration (right).

and a rectangular one, with beamwidth of $40\,^\circ$ in elevation, and respectively, $40\,^\circ$ and $20\,^\circ$ in azimuth. Dual (H and V) linear polarization is available, providing full-pol acquisitions (HH, HV, VH, and VV). The nominal antenna look-angle is $45\,^\circ$.

The radar operates at the central frequency of $1.3\,\mathrm{GHz}$, with an operating frequency range of 1.2–1.4 GHz. However, this large available radar bandwidth could not be exploited due to the authorization from the Belgian Institute for Post and Telecommunications being restricted to a bandwidth of $50\,\mathrm{MHz}$ centered on $1.375\,\mathrm{GHz}$. The pulse repetition frequency was $1004\,\mathrm{Hz}$ and the sampling frequency was $50\,\mathrm{MHz}$.

On each of the five flight missions, named F1 to F5, three parallel passes were necessary to cover the 4.5-km wide area, as depicted in Fig. 3. The flights were conducted along three overlapping tracks Zulu (Z), Alpha (A), and Bravo (B) in alternating opposite directions. A fourth short data sample, Z_{short}, was also acquired over a selected subset of the area of interest, incorporating the most numerous and representative fields (both maize and winter wheat), to perform a quick preliminary quality analysis of the data. Tracks A and B were flown from southwest to northeast, while Z and Z_{short} were covered from northeast

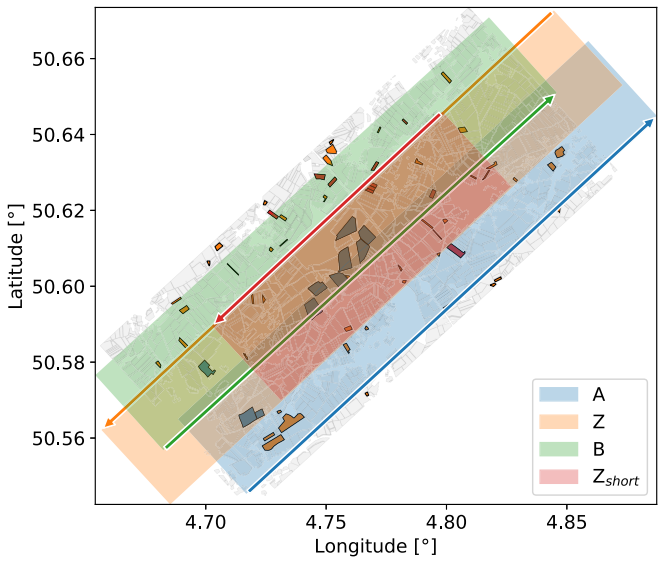

Fig. 3. Track design in alternating opposite directions to cover the BELSAR area of interest, and the subset area Z_{short}. The arrows indicate the trajectory of the left-looking sensors for each track.

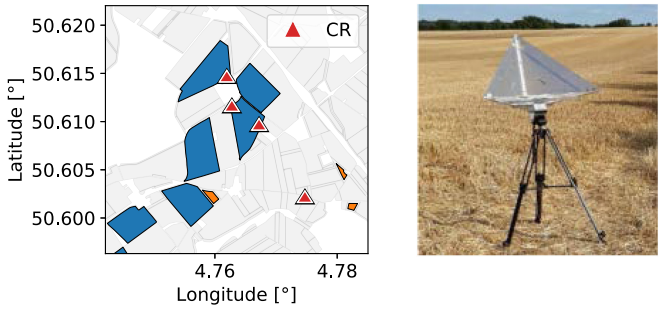

Fig. 4. Localization of the corner reflectors (CRs) within the subset area Z_{short} (left) and a CR in the field (right).

to southwest. It should be noted that the length of each track slightly varied from one flight to the other. Variations in size of the tracks from one flight to the next as well as their overlap resulted in some fields being imaged only on certain dates and others being imaged several times on the same day with different acquisition geometries. The latter were considered as different fields, and thus, separate data points in this study.

Four triangular pyramidal corner reflectors (CRs), depicted in Fig. 4, were deployed in the subset area, Z_{short}, and used for monostatic acquisitions to produce a geometrical reference as well as the point spread function (PSF), which provided the achieved resolutions and an indication about the quality of the synchronization between the transmitter and the receiver. They were located in a row in the across-track direction, spaced across one strip image, from near range to far range, remaining in the central part of it. Positions and azimuth orientation were determined for acquisition along the central track, Z. The elevation angle was adapted depending on the authorized altitude for each flight. The average flight altitude for each flight mission is provided in Table I. The position of the CRs was measured with a precision of $1\,\mathrm{m}$ using a GNSS receiver. They were

TABLE I
DATES (FORMAT: DAY-MONTH-2018) OF AIRBORNE SAR ACQUISITIONS AND CORRESPONDING *IN SITU* MEASUREMENTS (ISM), AND AVERAGE FLIGHT LEVELS OF THE FIVE BELSAR FLIGHT MISSIONS

Flight mission ID	Flight date	ISM date	Average flight level [m]
F1	30-05	30-05 and 31-05	2100
F2	20-06	21-06 and 22-06	2310
F3	30-07	01-08 and 02-08	2310
F4	28-08	29-08 and 30-08	2280
F5	10-09	10-09 and 11-09	2330

deployed and correctly aligned in azimuth and elevation for each flight.

On each flight mission, and for each track, mono- and bistatic data were acquired in two different bistatic geometries by flying the two airplanes carrying the multistatic system in tandem once in across-track (XT) and once in along-track (AT) flight configuration. Recommended values for both along-track and across-track baselines were established with the objective of keeping a convenient interferometric coherence range for interferometric applications. The small authorized frequency bandwidth and the quite low flight altitude drastically limited the critical baseline regarding geometric decorrelation and expected interferometric coherence [24]. Recommended XT baseline was then as short as $30\,\mathrm{m}$ at slightly different altitudes of about $5\,\mathrm{m}$ and with the master plane slightly behind the slave plane ($\sim 5\,\mathrm{m}$). In the case of the AT configuration, the along-track baseline constraint was dictated by the need for azimuthal spectra superposition, which imposed an along-track baseline of about a quarter of the flight altitude: 3-dB half width at mid antenna pattern is a little smaller than the flight altitude and decreases with decreasing range. Consequently, if considering an along track baseline of a fourth of the azimuthal footprint width at the mid antenna pattern, common intersection of azimuth spectra will be half the azimuth bandwidth only at high range. This intersection decreases at lower ranges leading to larger azimuthal resolution losses. Additionally, it also means that azimuthal filtering must be strongly range dependent to keep a good coherence. To avoid important azimuth resolution losses, but also to ease azimuth filtering while keeping a larger ground range swath available, it was suggested to limit the across-track baseline to one eighth of the 3-dB azimuth footprint width at mid antenna pattern, or around a quarter of the flying altitude.

The actual AT and XT baselines, respectively, were $450\,\mathrm{m}$ and about $35\,\mathrm{m}$ for all flight missions except for the first one (F1) in the AT configuration where an along-track baseline of about $900\,\mathrm{m}$ and a horizontal separation of about 60–80 m were observed [25]. This was much larger than expected. Ideally, there would have been no across-track separation and around $10\,\mathrm{m}$ in altitude separation. The actual baselines are shown on Fig. 5 for the first two flight missions, F1 and F2. These limited baselines, coupled with the fact that both SAR sensors were left-looking, strongly limited the scope of this study to measurements in the backward region with very small bistatic angles. Rather than bistatic, the resulting XT configuration could even rather be labeled as quasi-monostatic.

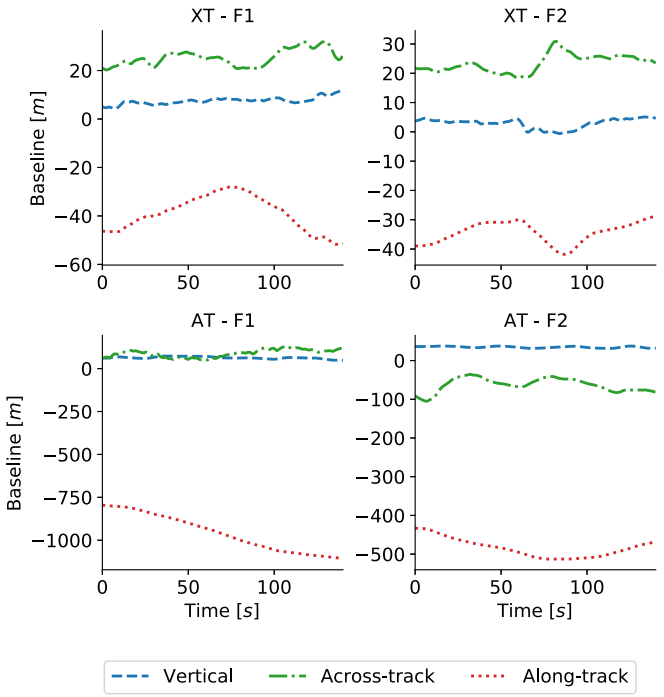

Fig. 5. Actual vertical, across-track, and along-track baselines between the sensors over Z_{short} for the first (F1; left) and second (F2; right) flight missions in the (top) XT and (bottom) AT flight configurations.

Radar data were processed by MetaSensing BV using the time-domain back-projection algorithm, which also handles motion compensation, and delivered as σ-calibrated single-look complex focused SAR data. Data were delivered in 320 ($=2$ sensors $\times$ 5 flights missions $\times$ 4 tracks $\times$ 2 bistatic configurations $\times$ 4 polarizations) NetCDF files composed of a series of arrays including the antenna pattern, navigation data, digital elevation model used, and position of the focused pixels in geographical coordinates (WGS84) [26]. Data were released in ground range geometry with a ground sampling distance of $1\,\mathrm{m}$. The images were coregistered based on the absolute position accuracy of the navigation data, which is around $0.75\,\mathrm{m}$, hence, less than pixel size.

The radiometric calibration providing the σ_0 was based on the CR response. The calibration constant K was evaluated for each flight mission. The same procedure was applied to mono- and bistatic data. For XT acquisitions, it was considered that the corner reflectors viewed by the bistatic acquisitions behaved similarly to the monostatic case. For bistatic data in the AT configuration, the corner reflectors are not present. The radiometric offset for the bistatic AT data is thus based on the monostatic AT and bistatic XT data. This might result in an imbalance between bistatic and monostatic, or from flight to flight, in the AT data.

A polarimetric calibration was also applied in order to insure the images acquired in the different polarization channels correctly reflect the dependence of the target response to the polarization state of the signal. Data were calibrated for co-pol and cross-pol channel imbalances, that is amplitude and relative phase differences between polarization channels, at both transmission and reception. Based on the obtained polarimetric signatures and CR impulse response function showing sufficiently good isolation between the polarizations at antenna level, cross-talk was considered negligible.

The radiometric and polarimetric calibration were performed according to the procedure described in [27].

In the context of this study, the acquisitions in the AT configuration suffer from two main problems. First, the spatial baseline between the sensors changed between the first flight mission, F1 ($900\,\mathrm{m}$), and the subsequent flight missions, F2–F5 ($450\,\mathrm{m}$). This had for consequence to make incomparable between them the images that resulted from the first and subsequent flights, and hence, to decrease significantly the quantity of data available for the analysis performed in this study. Then, and especially, the calibration of the bistatic images in AT had to be performed without the CRs, based on the monostatic acquisitions and those in XT. This may have resulted in imbalances. Images acquired in the XT configuration were not affected by those problems, hence, only those are considered in this study. A sample of these images can be seen on Fig. 6.

C. *In Situ Data*

The summer of 2018 was marked by an exceptional drought that impacted the campaign. Crops reached maturity early in the season and were consequently harvested several weeks earlier than usual. This limited the time window during which the crops could be observed and also resulted in unusually dry soil conditions.

Along with each flight mission, measurements of vegetation and soil biogeophysical variables were recorded in eight maize and ten winter wheat fields inside the imaged area. These fields are subsequently referred to as BELSAR reference fields and are reported in Fig. 2. The time series of the vegetation and soil biogeophysical variables collected *in situ* in these fields are represented in Fig. 7. In addition, the time series of their average mono- and bistatic scattering coefficients, acquired in the XT flight configuration, are depicted in Fig. 8. Finally, a summary of the airborne acquisitions dates and the corresponding *in situ* measurements dates can be found in Table I.

1) Maize Crop Variables: Maize crop biophysical variables were measured, up to the harvest, in three representative plots well inside the boundaries of each of the eight reference fields, and then, averaged at the field level. These plots were selected for their representativity according to their normalized difference vegetation index, which had been computed from Pleiades images days prior to the start of the campaign. For each of the three plots in each reference field, green area index (GAI) measurements were derived using the CAN-EYE software [28] from ten digital hemispheric pictures, one every $3.75\,\mathrm{m}$, with an approximate nadir view $1\,\mathrm{m}$ above the crop canopy. The GAI is an extension of the leaf area index (LAI) that includes not only the leaf area but also the stems and ears of the plants. It is, therefore, closer than the LAI to the actual biophysical variable being measured remotely [29]. In addition, plant height was measured with a ruler for nine different plants in each plot. Finally, the vegetation biomass was determined by destructive

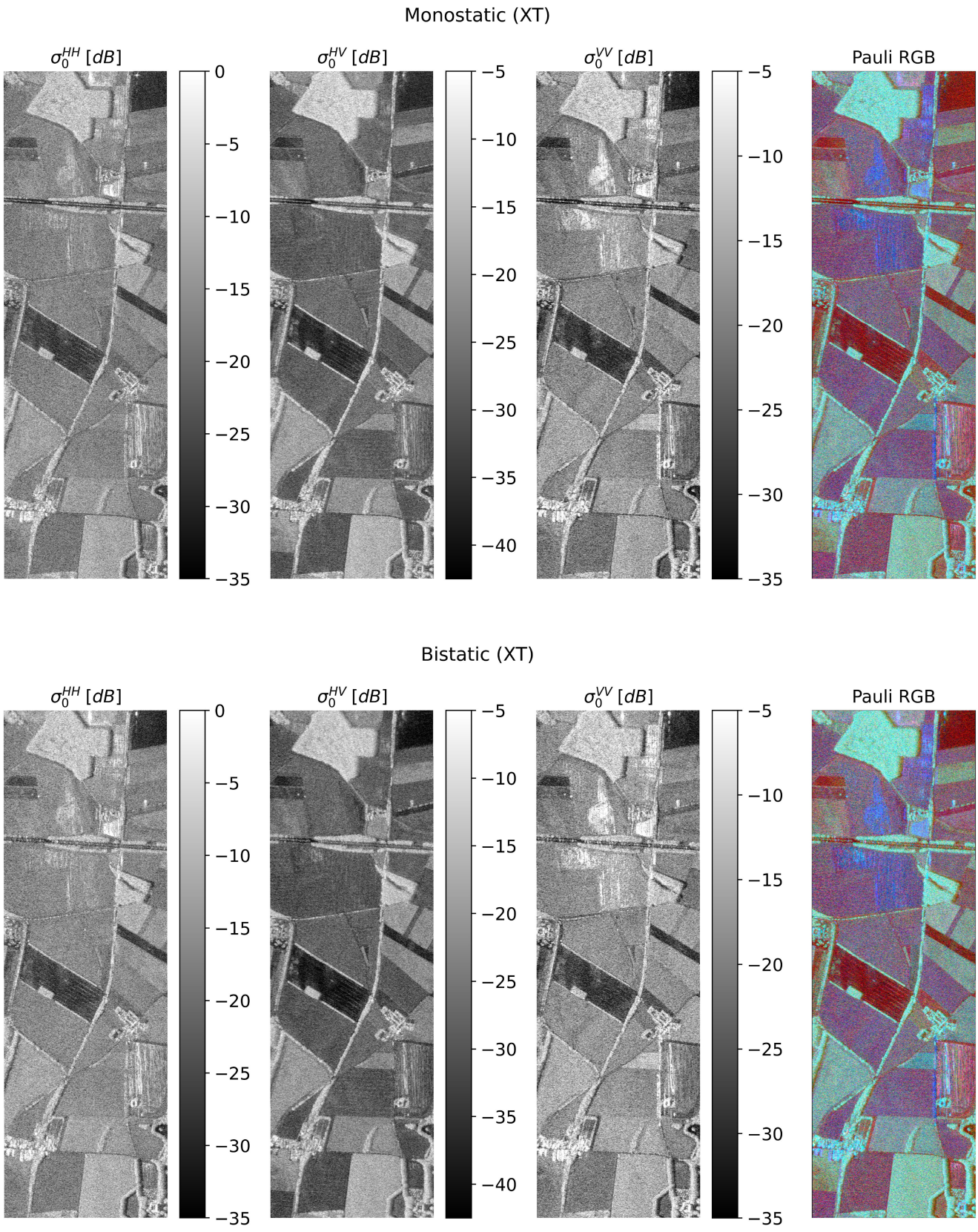

Fig. 6. (Top) Monostatic and (bottom) bistatic scattering coefficients σ_0 in HH, HV, and VV polarizations, as well as their Pauli RGB color composite (R: HH-VV; G: HV+VH; B: HH+VV), acquired on June 20 (F2) over a subset of the area covered by tracks Z and Z_{short} in the across-track (XT) bistatic configuration.

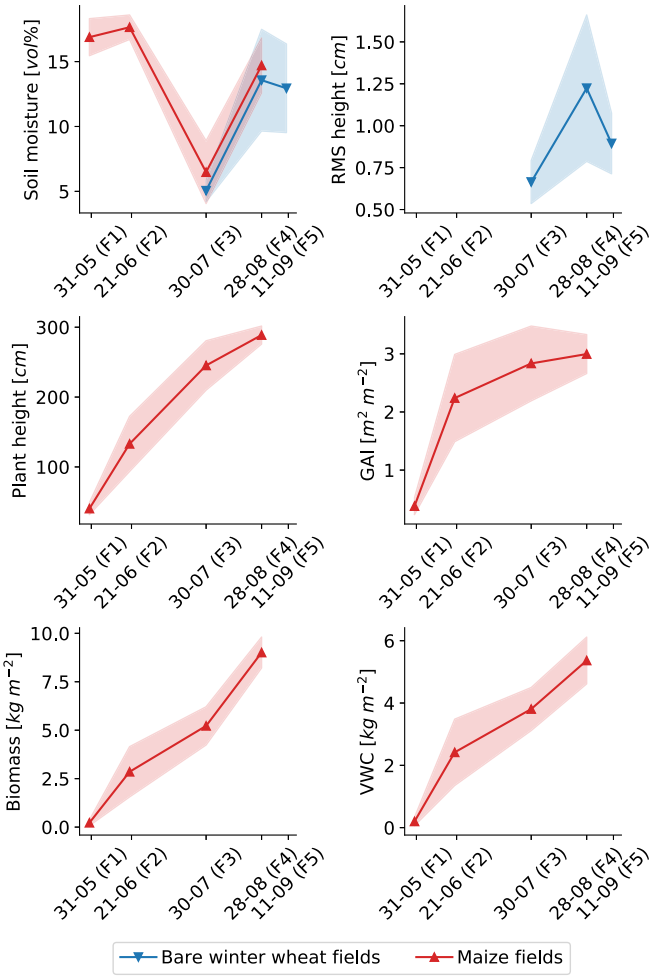

Fig. 7. Time series of the vegetation and soil biogeophysical variables measured *in situ* in the 18 BELSAR reference fields (eight maize and ten bare winter wheat). In red are the biophysical variables collected in the eight vegetated maize fields, i.e., plant height, vegetation biomass and water content (VWC), and green area index (GAI). In blue, the soil moisture and root mean square (rms) height from recently harvested winter wheat fields. The translucent areas represent two standard deviations around the mean.

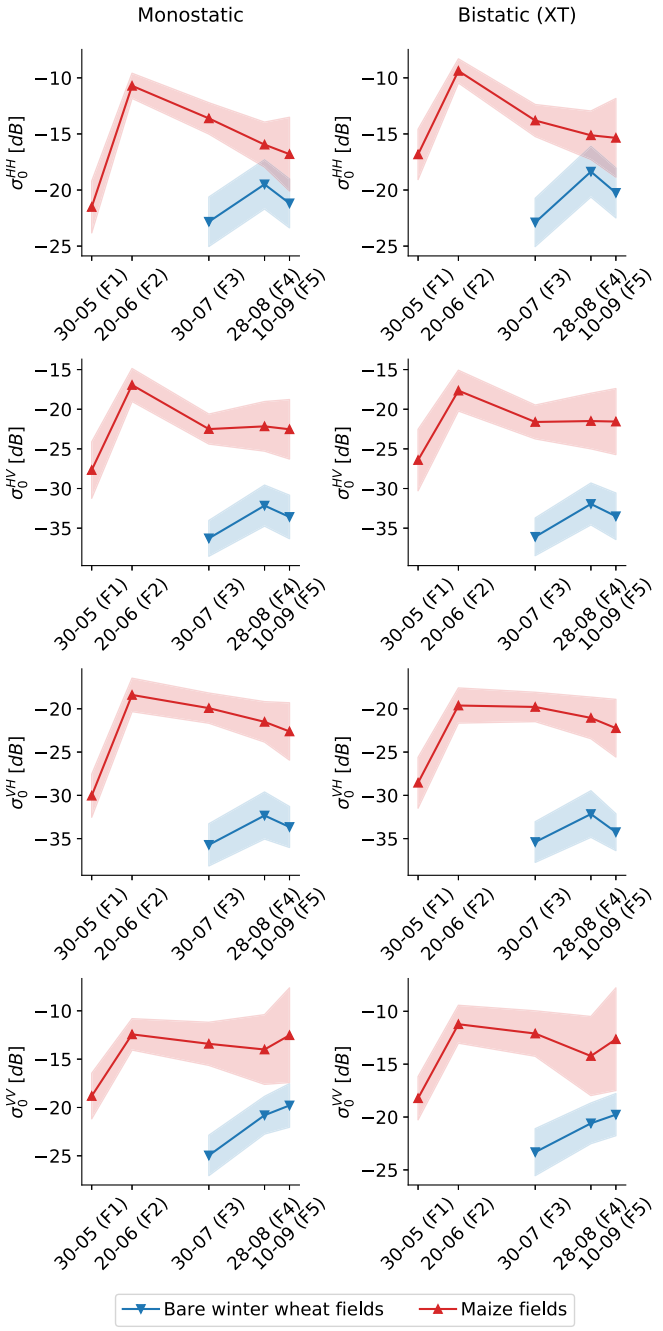

Fig. 8. Time series of the average monostatic (left) and bistatic scattering (right) coefficients σ_0 in HH, HV, VH, and VV polarizations (top to bottom), recorded in the BELSAR reference fields (eight maize and ten bare winter wheat), where the *in situ* measurements of vegetation and soil biogeophysical variables were collected. The translucent areas represent two standard deviations around the mean.

sampling and oven drying. In each plot, all the plants along three sowing lines of 1 m were harvested and weighted on the field to determine their fresh weight. A random subsample was then collected, weighted, and oven-dried in a microperforated bag at 60 °C for 72 h in order to determine their dry matter content, from which volumetric water content (VWC) was derived.

2) Below-Canopy and Bare Soil Variables: Soil moisture and surface roughness measurements were conducted in the harvested, and therefore, bare reference winter wheat fields, and only the former were recorded in the vegetated maize fields. Volumetric soil moisture measurements were conducted using time-domain reflectometry sensors with 11-cm rods. At least ten locations per reference field were monitored with three repetitions per location. All soil moisture measurements within each field were averaged to provide field average soil moisture values. The range of soil moisture values is 3.03–18.9vol%, which depicts very dry conditions, especially in July (F3). Soil surface roughness was determined using a pin profilometer of 1-m length, with a spacing of 1 cm. Roughness profiles along and across the direction of tillage were acquired to determine the root mean square (rms) height. At least five profiles per reference field were taken in both orientations on each acquisition date. Maize fields could not be monitored during their growing cycle. By means of linear regression analysis, it was found that the mean of rms height across and along the direction of tillage gives the best correlation with both mono- and bistatic scattering

signals and is, therefore, used in this study. The range of mean rms height measurements taken across and along the direction of tillage is 0.50–2.05 cm.

D. Row Orientation Data

The relative azimuth angle, i.e., the angle between the plane of incidence of the SAR sensor beam and the orientation of the planting rows, of 36 maize fields in the BELSAR area of interest was derived from high-resolution orthophotos. The fields were selected based on their size and shape so that their rows were straight and all oriented in the same direction. All but one of the BELSAR reference maize fields are part of this set.

The BELSAR area of interest, the ten winter wheat and eight maize fields for which *in situ* data are available, and these 36 maize fields, are all depicted in Fig. 2.

III. Methodology

The assessment of the sensitivity of the L-band mono- and bistatic SAR data to vegetation and soil biogeophysical variables is the subject of a separate methodology from the one used to assess their sensitivity to the vegetation row structure.

For the former, a linear regression analysis is performed to evaluate the sensitivity of the SAR measurements to the vegetation biophysical variables in maize crops, as well as to the surface soil moisture and roughness under the canopy in maize fields and in harvested (and therefore, bare) winter wheat fields. The aim is to compare the potential of simultaneous mono- and bistatic SAR data, which are referred to as multistatic in this study, with the traditional monostatic data for vegetation and soil monitoring applications.

For the latter, the canopy row structure effect is analyzed through the relationship between the orientation of the maize rows relative to the SAR sensor beam and the scattering measurements in almost all the imaged maize fields and at various phenological stages.

A. Vegetation Row Structure Effect

In order to assess the effect of the orientation of the rows of maize on the mono- and bistatic scattering measurements, a total of 36 sufficiently regular and large maize fields in the BELSAR area of interest are sorted into two groups according to the orientation of their rows relative to the SAR signal beam. The first group comprises fields that have a relative azimuth angle up to 30° departed from the plane of incidence of the signal beam. The second is made up of fields that have a relative azimuth angles between 0° and 30° or between 150° and 180°, i.e., (almost) perpendicular to the signal beam. The fields that belong to neither of the two aforementioned groups are discarded.

Assuming the normality of the samples, Welch's unequal variances *t*-tests [30] are then run for each SAR acquisition date to check whether the mean mono- and bistatic scattering coefficients of the two orientation groups are statistically distinct, which would suggest that the orientation of the rows relative to the signal beam has a significant impact on the scattering measurements.

B. Regression Analysis

To compare the potential of multistatic against monostatic scattering measurements for agriculture and soil monitoring, the mono- and bistatic scattering coefficients σ_0 (in power units) are first averaged at the field level for each polarization channel. Then, for every possible pair of polarizations, ratios of monostatic scattering coefficients as well as monostatic to bistatic scattering coefficients (so-called multistatic) are computed and converted to decibels. Next, the linear dependence of the monostatic scattering coefficients, the ratios of monostatic scattering coefficients, and the multistatic ratios on the vegetation and soil biogeophysical variable measured *in situ* are assessed via simple linear regression analysis. To that end, each biogeophysical variable measurement is temporally matched with each monostatic scattering coefficient, as well as with each mono- and multistatic ratio of scattering coefficients. Simple linear regression models are then fitted on the data via ordinary least squares, and the comparative performance of the models is quantified by their coefficients of determination

$$r^2 = 1 - \frac{\sum_{i=1}^{n}(y_i - \hat{y}_i)^2}{\sum_{i=0}^{n}(y_i - \bar{y})^2}$$

where y_i, $i = 1, \ldots, n$, are the observed scattering coefficients and ratios thereof, $\hat{y}_i$, $i = 1, \ldots, n$, are the predictions of the linear model, and $\bar{y}$ is the mean of the observations.

IV. Results and Discussion

A. Maize Row Orientation Effect

The fields of which the scattering coefficient measurements are discussed in this section are the 36 fields described in Section II-D. Except for the seven BELSAR reference maize fields that were measured *in situ*, no information is available on these maize fields other than their relative orientation to the SAR sensor beam.

It is very unlikely that these fields were harvested (in sufficient numbers) before July 30 (F3) and likely that the majority were harvested before August 20 (F4), based on the reference fields and farming practices in the region of interest. This analysis will, therefore, focus on the first three acquisitions (F1–F3).

Time series of average mono- and bistatic scattering coefficients for each orientation group are depicted on Fig. 9. The sample size of both orientation groups is similar for each acquisition date of interest, with 14 to 15 and 18 to 21 fields in each orientation group depending on the date. Furthermore, the acquisitions of the fields in each group have comparable incidence angle distributions and the maize crops show similar patterns of development. It is, therefore, very likely that the diverging behavior of the time series is mainly driven by the orientation of the maize rows relative to the signal beam.

The time series of monostatic and bistatic scattering coefficients are not significantly different from each other, except for the horizontal copolarization, HH, where the separation between the two orientation groups for the second and third acquisitions is slightly larger in bistatic than in monostatic mode.

Welch's *t*-tests performed for each acquisition date show that the two orientation groups significantly diverge from one another

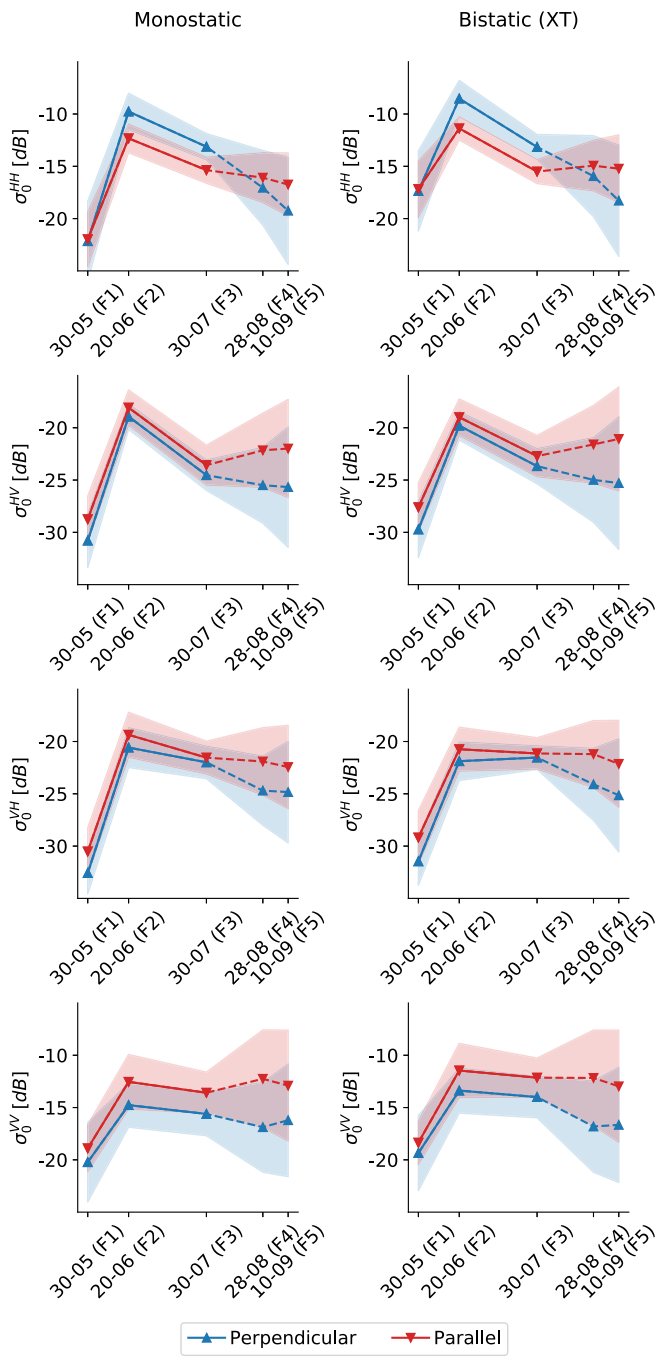

Fig. 9. Time series of the average monostatic (left) and bistatic (XT) scattering (right) coefficients σ_0 for each group of the 36 maize fields in the area of interest according to their orientation relative to the signal beam. The translucent areas represent two standard deviations around the mean. The harvest began after July 30 (F3), and it is highly likely that all fields were completely harvested by September 10 (F5). For the "perpendicular" group, the sample size is between 14 and 15 from F1 to F4 and 9 on F5. For the "parallel" group, the sample size is between 18 and 21.

on June 20 (F2) and July 30 (F3), in both copolarizations, HH and VV, but especially in the former. Before that, on May 30 (F1), both orientation groups are indistinguishable from one another in HH or VV, probably because the crop is still underdeveloped. After July 30 (F3), the maize fields are harvested gradually until mid September (F5). In HV, VH, and VV polarizations, the mean mono- and bistatic scattering coefficients for the group with fields the rows of which are (almost) parallel to the sensor beam is larger than that of the group with fields the rows of which are (almost) perpendicular to it, for each acquisition date. This is more likely related to the sampling rather than to an effect of the rows since this difference persists beyond harvest, when the fields are bare except for stem residues. In horizontal copolarization, HH, however, for the second (F2) and third (F3) acquisitions, fields with rows perpendicular to the SAR sensor beam have a higher values of scattering coefficients than those the rows of which are parallel to it. This does not hold true for the first (F1) acquisition, when the crop is not yet fully developed, nor for the fourth (F4) and fifth (F5) acquisitions, which take place after the beginning of the harvest.

These observations seem to point to an effect of the relative orientation of the maize rows, and thus, the row structure of the canopy, in both HH and VV, but that is far more pronounced in the former, while for the cross polarizations, HV and VH, no effect is discernible.

These results are consistent with other studies on the effect of row orientation on backscatter measurements. In their experimental study on the effect of sugarcane planting row direction on ALOS/PALSAR (L-band) imagery, Picoli *et al.* [31] report that, in HH, the values of backscattering coefficient are higher for fields with perpendicular rows than for those with parallel rows. For HV, however, they find no statistically significant effect of the planting row direction. Multiple theoretical investigations have also shown that the row orientation has a significant effect on backscatter measurements in copolarization, and especially, in HH, e.g., [32]–[34]. However, in these model-based studies, qualitatively similar behaviors are reported for HH and VV, which is not apparent here. Regarding the impact of the row structure of crops on bistatic radar measurements, there is, to our knowledge, no published study on the subject.

B. Sensitivity to Soil Moisture and Roughness in Bare Fields

The linear sensitivity of both monostatic and multistatic radar systems to soil moisture is assessed in recently harvested, and hence, bare winter wheat fields. Fig. 10 depicts the coefficients of determination (r^2) of the simple linear regression models fitted on the radar and biogeophysical measurements.

Monostatic scattering coefficients in co- and cross-polarizations (HH, HV, VH, and VV) are linearly sensitive to soil moisture in bare fields, i.e., the field average monostatic scattering coefficients increase with soil moisture. A relatively high correlation is found for VV, in particular, with an r^2 score of $40\,\%$. However, all four monostatic scattering coefficients also show high r^2 scores for surface roughness, which might indicate that the signal is sensitive to it as well as to soil moisture, as depicted in Fig. 11. This makes the soil moisture retrieval from monostatic observations challenging, particularly in the horizontal copolarization, HH, for which a relatively high r^2 score of $46\,\%$ is found for the surface roughness.

In general, ratios of monostatic scattering coefficients have near-zero r^2 scores for surface roughness, which suggests a reduced sensitivity to it compared to the monostatic scattering

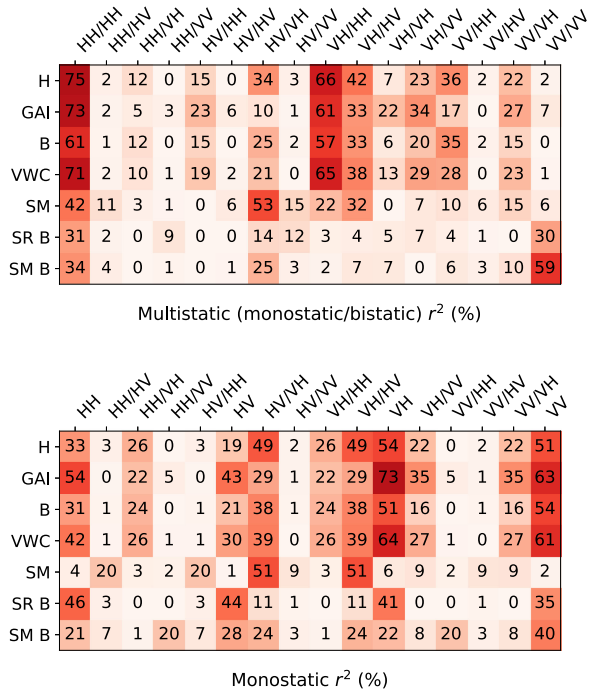

Fig. 10. Coefficients of determination, r^2 (%), of simple linear regressions between multistatic ratios (top), i.e., ratios of monostatic to bistatic (XT) scattering coefficients, monostatic scattering coefficients and their ratios (bottom), and for maize crops, plant height (H; $n = 26$), green area index (GAI; $n = 26$), biomass (B; $n = 26$), vegetation water content (VWC; $n = 26$), soil moisture under canopy (SM; $n = 26$), as well as, for bare winter wheat fields, soil moisture (SM B; $n = 36$) and mean rms height (SR B; $n = 37$).

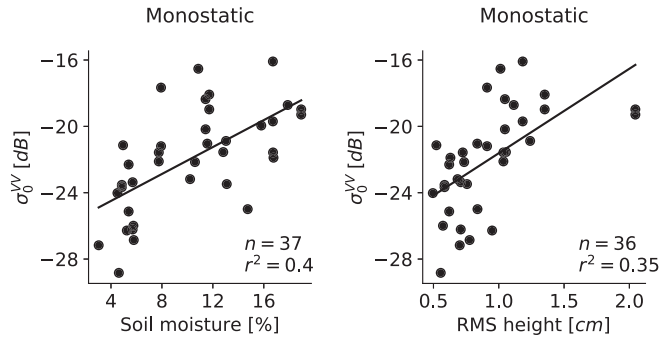

Fig. 11. Scatter plots of the monostatic scattering coefficient σ_0 in VV as a function of the volumetric soil moisture (left) and rms height (right) measured in situ in the BELSAR reference winter wheat fields after the harvest (bare).

coefficients in HH, HV, VH, and VV, and comparable sensitivities between mono- and bistatic measurements. Furthermore, the ratios of co- and cross-polarized monostatic scattering coefficients HH/VV and HV/VH (and VV/HH and VH/HV respectively, by symmetry) show relatively high r^2 scores for soil moisture, with $r^2 = 20\,\%$ and $r^2 = 24\,\%$, respectively, and low ones for surface roughness, especially for HH/VV. These ratios of monostatic scattering coefficients, thus, seem to be relatively sensitive to soil moisture but not at all to surface roughness. This would suggest that using monostatic scattering observations in two polarizations simultaneously might mitigate the impact of surface roughness in soil moisture retrieval. As for the ratios of scattering coefficients of the multistatic radar system, they also show low r^2 scores for surface roughness. However, the r^2 scores for soil moisture are low as well. Only for the multistatic ratios HH/HH and VV/VV are the r^2 score for soil moisture relatively high, with $r^2 = 34\,\%$ and $r^2 = 59\,\%$, respectively. Unfortunately, the r^2 score for the surface roughness is also high for these. This suggests that the bistatic radar configuration of the BELSAR campaign might not be suitable for soil moisture retrieval over bare fields.

It should be noted that the BELSAR bistatic observations were only available in the backward region and not in the more theoretically promising forward region and that bistatic angles between transmitting and receiving antennas were very small. Given this, it was expected that the bistatic SAR data would not provide more useful information on soil moisture retrieval than traditional monostatic observations.

C. Sensitivity to Vegetation and Soil Biogeophysical Variables

In vegetated maize fields, the coefficients of determination suggest that the multistatic system might be more sensitive to the vegetation biophysical variables compared to the monostatic one. The multistatic system does indeed allow predicting, from the best performing polarization ratio for each vegetation variable, 75%, 73%, 61%, and 71 % (all in HH/HH) of the variance in maize plant height, green area index, biomass, and vegetation water content, outperforming the monostatic system by 20% (VH), 7% (VV), and 7 % (VH) for each biophysical variable except the GAI, respectively. With regards to the soil moisture under the canopy, both the monostatic and the multistatic systems have similar r^2 scores, respectively, 51% (HV and VH) and 53 % (HV/VH), but they are significantly lower than the scores for the canopy variables. This might be caused by the attenuation of the signal by the vegetation.

For the monostatic system, the vertical co- and cross-polarizations, VV and VH, have similar performances and significantly outperform all other polarizations and ratios thereof. For its multistatic counterpart, however, the best choice for maize monitoring would be the ratio of horizontally copolarized monostatic to bistatic scattering coefficients HH/HH, followed by VH/HH. It is noteworthy that the vertical polarization VV does not seem to bring any gain in terms of sensitivity to vegetation variables to the multistatic system.

The multistatic ratios, HV/HV, VH/VH, and VV/VV, have near-zero r^2 for all maize biophysical parameters, as well as for the surface soil moisture under the canopy. This indicates that the ratios are (almost) constant, and thus, the information content of mono- and bistatic acquisitions is the same for HV, VH, and VV. Conversely, in HH polarization, bistatic acquisitions seem to increase the information content of the system compared to monostatic acquisitions alone. For example, Fig. 12 illustrates the impact that the addition of a bistatic component to the system, via its use in a ratio, has on the relationship between maize plant height and radar measurements in horizontal copolarization. This suggests that in HH, the acquisitions have a greater dependence in the acquisition geometry of the sensors forming the bistatic system than the other polarizations. These results are, therefore, in agreement with the results of the analysis

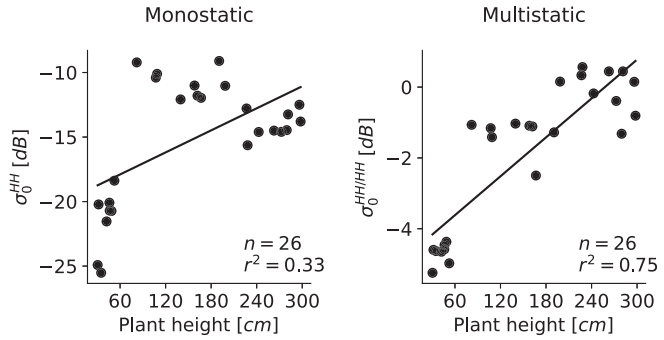

Fig. 12. Scatter plots of the monostatic scattering coefficient σ_0 in HH (left) and the (multistatic) ratio of monostatic to bistatic scattering coefficients in HH (right) as a function of the plant height measured in situ in the BELSAR reference maize fields.

of the effect of the vegetation row structure in Section IV-A, which show that measurements in horizontal copolarization, HH, are significantly more impacted by the anisotropy of the target induced by the row structure of the vegetation canopy.

Finally, discrepancies between the coefficients of determination reported in Fig. 10 for the cross-polarization channels, HV and VH, of the monostatic system suggest that the reciprocity theorem does not hold true for vegetated maize fields. It does seem to be valid to a reasonable degree, however, for bare soils in harvested winter wheat fields. The reason for this difference between vegetated and bare fields might be due to the theorem being only valid for quiet environments, an assumption that is not always verified in real conditions, as also reported in [35], or because of the anisotropic nature of the target [3].

V. Conclusion

In this study, we assessed the potential of multistatic SAR for crop and soil moisture monitoring. The results suggest that multistatic SAR systems are more sensitive to maize crop biophysical variables than purely monostatic ones, even with very short bistatic angles and baselines. This is attributed to the row structure of the vegetation in maize fields. The analysis of the effect of the maize row orientation relative to the SAR sensor beam has indeed shown a significant impact of the row planting direction on the mono- and bistatic scattering measurements in L-band in both copolarizations, but especially in HH, as soon as the stem elongation phase. With regards to the soil moisture and surface roughness of bare soils, however, the simultaneous use of mono- and bistatic scattering data does not appear to provide additional information that would enable the disentanglement of their respective contributions.

The results of this assessment were derived from data acquired with a very small bistatic angle ($\sim 1^\circ$), i.e., in a quasi-monostatic configuration. From theoretical studies on the scattering properties of vegetation and soil, however, it is expected that multistatic systems with considerably larger bistatic baselines and angles could significantly improve the accuracy of vegetation and soil biogeophysical variables retrieval [3]. A larger dataset with a greater range of acquisition geometries would thus be needed to draw general conclusions about the performance of multistatic systems for applications in agriculture and soil monitoring.

Acknowledgment

The authors would like to thank the BELSAR-Campaign team for the collection of the joint airborne SAR and *in situ* datasets used in this work, as well as Prof. L. Guerriero from the Tor Vergata University of Rome, Prof. N. Pierdicca from the Sapienza University of Rome, and Prof. H. Griffiths from University College London, for participating in their scientific exploitation.

References

[1] A. Della Vecchia *et al.*, "Optimization of bistatic radar configurations for vegetation monitoring," in *Proc. IEEE Int. Symp. Geosci. Remote Sens.*, 2006, pp. 1220–1223.

[2] L. Guerriero, N. Pierdicca, L. Pulvirenti, and P. Ferrazzoli, "Use of satellite radar bistatic measurements for crop monitoring: A simulation study on corn fields," *Remote Sens.*, vol. 5, no. 2, pp. 864–890, 2013.

[3] N. Pierdicca, M. Brogioni, F. Fascetti, J. D. Ouellette, and L. Guerriero, "Retrieval of biogeophysical parameters from bistatic observations of land at L-band: A theoretical study," *IEEE Trans. Geosci. Remote Sens.*, vol. 60, May 2021, Art. no. 4402517.

[4] T. Schmugge, "Remote sensing of soil moisture: Recent advances," *IEEE Trans. Geosci. Remote Sens.*, vol. GE-21, no. 3, pp. 336–344, 1983.

[5] F. T. Ulaby, *Microwave Remote Sensing Active and Passive*. Norwood, MA, USA: Artech House, 1982.

[6] F. T. Ulaby, R. K. Moore, and A. K. Fung, *Microwave Remote Sensing: Active and Passive, From Theory to Applications*, vol. 3. Norwood, MA, USA: Artech House, 1986.

[7] L. Rakotoarivony, O. Taconet, D. Vidal-Madjar, P. Bellemain, and M. Benallegue, "Radar backscattering over agricultural bare soils," *J. Electromagn. Waves Appl.*, vol. 10, no. 2, pp. 187–209, 1996.

[8] N. E. Verhoest, H. Lievens, W. Wagner, J. Álvarez-Mozos, M. S. Moran, and F. Mattia, "On the soil roughness parameterization problem in soil moisture retrieval of bare surfaces from synthetic aperture radar," *Sensors*, vol. 8, no. 7, pp. 4213–4248, 2008.

[9] A. Allies *et al.*, "Evaluation of multiorbital SAR and multisensor optical data for empirical estimation of rapeseed biophysical parameters," *IEEE J. Sel. Topics Appl. Earth Observ. Remote Sens.*, vol. 14, pp. 7268–7283, Jul. 2021.

[10] N. Efremova, M. E. A. Seddik, and E. Erten, "Soil moisture estimation using Sentinel-1/-2 imagery coupled with cycleGAN for time-series gap filing," *IEEE Trans. Geosci. Remote Sens.*, vol. 60, Dec. 2021, Art. no. 4705111.

[11] Y. Liu, J. Qian, and H. Yue, "Combined Sentinel-1 A with Sentinel-2 A to estimate soil moisture in farmland," *IEEE J. Sel. Topics Appl. Earth Observ. Remote Sens.*, vol. 14, pp. 1292–1310, Dec. 2020.

[12] P. Ferrazzoli, L. Guerriero, C. I. Del Monaco, and D. Solimini, "A further insight into the potential of bistatic SAR in monitoring the Earth surface," in *Proc. IEEE Int. Geosci. Remote Sens. Symp.*, 2003, vol. 2, pp. 776–777.

[13] N. Pierdicca, L. Pulvirenti, F. Ticconi, and M. Brogioni, "Radar bistatic configurations for soil moisture retrieval: A simulation study," *IEEE Trans. Geosci. Remote Sens.*, vol. 46, no. 10, pp. 3252–3264, Oct. 2008.

[14] N. Pierdicca, L. De Titta, L. Pulvirenti, and G. D. Pietra, "Bistatic radar configuration for soil moisture retrieval: Analysis of the spatial coverage," *Sensors*, vol. 9, no. 9, pp. 7250–7265, 2009.

[15] M. Brogioni *et al.*, "Sensitivity of bistatic scattering to soil moisture and surface roughness of bare soils," *Int. J. Remote Sens.*, vol. 31, no. 15, pp. 4227–4255, 2010.

[16] J. T. Johnson and J. D. Ouellette, "Polarization features in bistatic scattering from rough surfaces," *IEEE Trans. Geosci. Remote Sens.*, vol. 52, no. 3, pp. 1616–1626, Mar. 2013.

[17] J. Zeng and K.-S. Chen, "Theoretical study of global sensitivity analysis of L-band radar bistatic scattering for soil moisture retrieval," *IEEE Geosci. Remote Sens. Lett.*, vol. 15, no. 11, pp. 1710–1714, Nov. 2018.

[18] A. Egido *et al.*, "Global navigation satellite systems reflectometry as a remote sensing tool for agriculture," *Remote Sens.*, vol. 4, no. 8, pp. 2356–2372, 2012.

[19] M. Zribi *et al.*, "Potential applications of GNSS-R observations over agricultural areas: Results from the GLORI airborne campaign," *Remote Sens.*, vol. 10, no. 8, 2018, Art. no. 1245.
[20] J. Zeng, K.-S. Chen, H. Bi, Q. Chen, and X. Yang, "Radar response of off-specular bistatic scattering to soil moisture and surface roughness at l-band," *IEEE Geosci. Remote Sens. Lett.*, vol. 13, no. 12, pp. 1945–1949, Dec. 2016.
[21] J. Bouchat, E. Tronquo, H. Lievens, N. Verhoest, and P. Defourny, "Assessing the potential of fully-polarimetric simultaneous mono-and bistatic airborne SAR acquisitions in L-band for applications in agriculture and hydrology," in *Proc. IEEE Int. Geosci. Remote Sens. Symp.*, 2021, pp. 2703–2706.
[22] J. Bouchat and P. Defourny, "Effect of row orientation on maize green area index retrieval from L-band synthetic aperture radar imagery," in *Proc. IEEE Int. Geosci. Remote Sens. Symp.*, 2021, pp. 6716–6719.
[23] K. A. C. de Macedo, S. Placidi, and A. Meta, "Bistatic and monostatic InSAR results with the MetaSensing airborne SAR system," in *Proc. 6th Asia-Pacific Conf. Synthetic Aperture Radar*, 2019, pp. 1–5.
[24] A. Orban, D. Defrere, and C. Barbier, "BelSAR: The first Belgian airborne campaign for L-band, full polarimetric bistatic and interferometric SAR acquisitions over an agricultural site in Belgium," in *Proc. 13th Eur. Conf. Synthetic Aperture Radar*, 2021, pp. 1–4.
[25] Centre spatial de Liège, "BelSAR data acquisition report," Centre spatial de Liège, Angleur, Belgium, Tech. Rep. RP-CSL-BEL-18006, Jan. 2019.
[26] MetaSensing BV, "MetaSAR-L NetCDF, file format description," MetaSensing BV, Noordwijk, Netherlands, Tech. Rep. MS-CSL-BEL-FFD-002-13, Jul. 2019.
[27] A. G. Fore *et al.*, "UAVSAR polarimetric calibration," *IEEE Trans. Geosci. Remote Sens.*, vol. 53, no. 6, pp. 3481–3491, Jun. 2015.
[28] M. Weiss and F. Baret, *CAN-EYE V6.4.91 User Manual*, p. 56, 2017. [Online]. Available: https://hal.inrae.fr/hal-02788819
[29] G. Duveiller, M. Weiss, F. Baret, and P. Defourny, "Retrieving wheat green area index during the growing season from optical time series measurements based on neural network radiative transfer inversion," *Remote Sens. Environ.*, vol. 115, no. 3, pp. 887–896, 2011.
[30] B. L. Welch, "The generalization of 'students's' problem when several different population variances are involved," *Biometrika*, vol. 34, no. 1-2, pp. 28–35, 1947.
[31] M. C. A. Picoli, R. A. C. Lamparelli, E. E. Sano, J. R. B. de Mello, and J. V. Rocha, "Effect of sugarcane-planting row directions on ALOS/PALSAR satellite images," *GISci. Remote Sens.*, vol. 50, no. 3, pp. 349–357, 2013.
[32] A. Sharma, R. H. Lang, M. Kurum, P. E. O'Neill, and M. H. Cosh, "L-band radar experiment and modeling of a corn canopy over a full growing season," *IEEE Trans. Geosci. Remote Sens.*, vol. 58, no. 8, pp. 5821–5835, Aug. 2020.
[33] U. Wegmüller *et al.*, "Progress in the understanding of narrow directional microwave scattering of agricultural fields," *Remote Sens. Environ.*, vol. 115, no. 10, pp. 2423–2433, 2011.
[34] M. Zribi, O. Taconet, V. Ciarletti, and D. Vidal-Madjar, "Effect of row structures on radar microwave measurements over soil surface," *Int. J. Remote Sens.*, vol. 23, no. 24, pp. 5211–5224, 2002.
[35] F. Totir *et al.*, "Recent polarimetric SAR models for Danube Delta monitoring using PALSAR images," in *Proc. 5th Int. Workshop Sci. Appl. SAR Polarimetry Polarimetric Interferometry*, 2011, pp. 1–8.

Jean Bouchat received the master's degree in mathematical engineering in 2019 from Université catholique de Louvain (UCLouvain), Louvain-la-Neuve, Belgium, where he is currently working toward the Ph.D. degree with the Geomatics Research Laboratory, Earth and Life Institute.

His research interests include radar remote sensing for agriculture monitoring.

Emma Tronquo was born in Asse, Belgium. She received the M.Sc. degree in applied biological sciences from Ghent University, Ghent, Belgium, in 2019.

She is currently a Doctoral Researcher with the Hydro-Climate Extremes Lab (H-CEL), Ghent University. Her main research interests include soil moisture retrieval from active microwave sensing and hydrologic modeling.

Anne Orban was born in Brussels, Belgium. She received the M.Sc degree in physiscs in 1986 and the specialized master's degree in ionizing radiation and radioprotection in 1987, from Université catholique de Louvain (UCLouvain), Belgium.

Since 1988, she has been working with the Centre Spatial de Liège then named IAL Space, first with the Space Environment Group, then with the Signal Processing Laboratory, where she began to be active in the field of synthetic aperture radar (SAR) and whom she has been responsible since 2017. Her main research interests include remote sensing and Earth observation, including development of SAR processing tools and InSAR, PolSAR, and PolInSAR applications.

Niko E. C. Verhoest received the B.E. and Ph.D. degrees in applied biological sciences from Ghent University, Ghent, Belgium, in 1994 and 2000, respectively.

He was a Teaching Assistant and an Assistant Professor with the Laboratory of Hydrology and Water Management (currently Hydro-Climate Extremes Lab), Ghent University, from 1998 to 2000 and 2000 to 2002, respectively. In 2002, he became an Associate and Full Professor of hydrology and water management with the Faculty of Bioscience Engineering, Ghent University. His research interests include hydrological applications of radar remote sensing.

Pierre Defourny (Member, IEEE) received the Ph.D. degree in agricultural engineering from the Université catholique de Louvain (UCLouvain), Louvain-la-Neuve, Belgium, in 1992.

He spent several years in remote sensing research in Africa, Southeast Asia, and Central America. He is the Founding President of the Earth and Life Institute. He is currently a Full Professor with UCLouvain. He also leads the Geomatics Research Laboratory with a special focus on open source system development to exploit Sentinel missions for agriculture and forestry monitoring. His research interests include developing monitoring systems of land cover/land-use change across spatial and temporal scales.